Mechanical Analysis of Idealized Shallow Hydraulic Fracture

Lawrence C. Murdoch[1]

Abstract: The characteristics of hydraulic fractures created at shallow depths are known from excavations and borings, but this understanding has lagged behind the ability to predict fracture growth. This paper describes a simple analysis based on elasticity theory and fracture mechanics that will predict characteristics of shallow hydraulic fractures that are relatively flat lying. The analysis gives closed-form expressions for the injection pressure, fracture aperture, and radial length as functions of time, fracture toughness, and elastic modulus. The analysis is first used to estimate fracture toughness and elastic modulus of shallow formations from field tests of hydraulic fracturing. Those parameters are used to calibrate the model and predict the growth of fractures. The average relative error of the predictions is about 20% and increases with the dip and degree of asymmetry of the fracture.

DOI: 10.1061/(ASCE)1090-0241(2002)128:6(488)

CE Database keywords: Fractures; Mechanic properties; Hydraulics.

Introduction

Hydraulic fractures created at shallow depths have been used to improve the performance of environmental remediation projects involving subsurface flow (Murdoch et al. 1995), and they are the basis for the creation of chemically reactive barriers designed to inhibit contaminant migration in the vadose zone (Murdoch 2000). Hydraulic fractures are recognized as a potential problem during some grouting operations (Morgenstern and Vaughn 1963; Wong and Farmer 1973), but in other cases fractures with forms similar to those used for environmental applications have improved the performance of grouting procedures (Caron 1982; Chandler 1997). Injection-based well testing to determine formation properties may be confounded if hydraulic fractures are created inadvertently (Bjerrum et al. 1974).

The details of some hydraulic fractures created at shallow depths are known because they can be scrutinized in excavations and borings (Murdoch 1988, 1989, 1995), but this understanding has lagged behind the ability to predict fracture growth. An overview of the characteristics of shallow hydraulic fractures has been described in a companion paper (Murdoch and Slack 2002) that appears in this issue. The purpose of this paper is to present an analysis that is able to predict aspects of the growth of shallow hydraulic fractures created for environmental purposes and described by Murdoch and Slack (2002).

Methods for analyzing hydraulic fractures are well established from more than 50 years of investigations by workers in the petroleum industry where hydraulic fractures have long been used to increase the yields of oil wells. Analyses published by petroleum engineers are extensive and reviews can be found in Gidley et al. (1989), Veatch (1983a,b), and Murdoch (1991). Highly sophisticated codes that predict the characteristics of hydraulic fractures in oil reservoirs are currently available, but most of them will provide limited insights into characteristics of the shallow hydraulic fractures described by Murdoch and Slack (2002). This shortcoming occurs largely because hydraulic fractures in oil reservoirs are vertical and fail to interact with the ground surface, whereas the fractures described by Murdoch and Slack (2002) are gently dipping and interact strongly with the ground surface. Perkins and Kern (1961) present an analysis of a flat-lying circular hydraulic fracture in an oil reservoir, and aspects of their analysis are similar to the one described here.

The process of hydraulic fracturing has been used as an analogy to the growth of igneous intrusions (Pollard 1973; Pollard and Johnson 1973; Pollard 1978). Sills are igneous intrusions that are parallel to bedding and they are commonly flat-lying to gently dipping, and laccoliths are igneous intrusions that strongly interact with the ground surface. As a result, analyses that have been applied to understand sills and laccoliths have characteristics that are important to understanding shallow, flat-lying hydraulic fractures. Those analyses will be modified, however, to include a propagation criteria that appears to be relevant for shallow sediments, and to include conditions that pertain to the hydraulic fracturing process, such as a fluid balance on the fracture.

The growth of dilational, or mode I, fractures in fine-grained soils can be predicted using methods of linear elastic fracture mechanics, according to Morris et al. (1994), Vallejo and Liang (1994), Harison et al. (1994) and Murdoch (1993a,b,c). The use of a critical mode I stress intensity, K_{IC}, or a related parameter as a criteria for propagation is central to the application of linear elastic fracture mechanics. Murdoch (1993a,b,c) has shown that analyses based on fracture mechanics and the use of K_{IC} in particular are capable of predicting the essential details of hydraulic fractures created in blocks of silty clay in the laboratory. The analysis described here will build on the previous work described both by petroleum engineers and investigators in geomechanics.

The typical hydraulic fracture in shallow, fine-grained formations is a gently dipping feature that is slightly asymmetric with

[1]Assistant Professor, Dept. of Geological Sciences, Clemson Univ., Clemson, SC 29634. E-mail: lmurdoch@clemson.edu

Note. Discussion open until November 1, 2002. Separate discussions must be submitted for individual papers. To extend the closing date by one month, a written request must be filed with the ASCE Managing Editor. The manuscript for this paper was submitted for review and possible publication on October 23, 2000; approved on September 6, 2001. This paper is part of the *Journal of Geotechnical and Geoenvironmental Engineering*, Vol. 128, No. 6, June 1, 2002. ©ASCE, ISSN 1090-0241/2002/6-488–495/$8.00+$.50 per page.

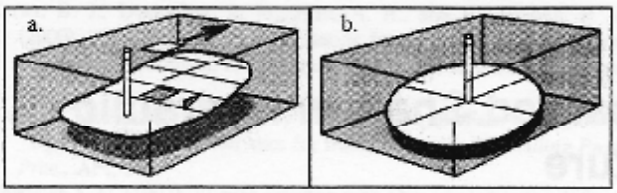

Fig. 1. (a) Typical hydraulic fracture inferred from field measurements. (b) Idealized circular form used to represent hydraulic fracture in the analyses.

respect to its parent borehole (Fig. 1), according to the paper by Murdoch and Slack (2002). This typical fracture grows primarily radially, although many have a preferred direction of propagation so they grow in one radial direction more than the others. The maximum length of these features is several times greater than their depth, and the aperture of the fractures is two to three orders of magnitude less than their maximum length.

Analyzing the form of the typical hydraulic fracture shown in Fig. 1(a) will require a three-dimensional analysis that currently can only be conducted using a state-of-the-art numerical simulator such as the one described by Carter et al. (2002). However, it is possible to infer an idealized form that captures important features of the field observations while retaining a geometric simplicity that can be solved analytically. It is the purpose of this paper to develop such an idealized model and to evaluate the model by comparing the results it predicts to observations from the field. This exercise is intended to be a first step that will lead the way for more detailed numerical analyses in the future.

Conceptual Model

A hydraulic fracture at shallow depths will be analyzed as a horizontal, circular, disk-shaped cavity loaded by internal fluid pressure and embedded in an elastic medium [Fig. 1(b)]. This feature resembles the actual idealized fracture (Fig. 1), but there are a variety of geometric differences which will be examined individually in the following section.

Dip

Field observations show that many hydraulic fractures in shallow, fine-grained deposits dip less than 20° and some fractures are within a few degrees of horizontal (Murdoch and Slack 2002, Figs. 2 and 3). It seems reasonable to ignore the effect of dip and simply assume as a first approximation that fractures dipping less than 20° can be represented as flat lying.

The dip of hydraulic fractures at some locations is greater than 20° and it may be nearly vertical. The analysis developed here will be inapplicable to those steeply dipping fractures. However, hydraulic fractures with relatively gentle dips appear to be common and they have more environmental applications than their steeply dipping counterparts, so this limitation will be acceptable.

Aspect Ratio

The average plan aspect ratio of gently dipping hydraulic fractures is 1.2, that is, one axis is 20% longer than the other (Murdoch and Slack 2002, Fig. 9). The point of maximum uplift and the point of injection are both eccentric with respect to the center of the fracture in plan. On average, the point of maximum uplift and the point of injection differ from the center of the fracture by a distance that is 14% of the major axis, according to Murdoch and Slack (2002). Both the elongate aspect ratio and the eccentric location of the maximum uplift and injection well are clearly recognizable features of shallow hydraulic fractures, but their average magnitude appears to differ from the idealized, symmetric form by an amount that is small relative to the size of the fractures. Ignoring these geometric features appears to be warranted based on their magnitude, although this assumption should be tested when a three-dimensional model is available.

Dilation

The walls of a gently dipping hydraulic fracture will be displaced either by compressing the adjacent material or by lifting the overburden, or a combination of the two mechanisms. The ratio of fracture length to depth determines the extent of the contribution of each mechanism, with compression favored when the ratio is small and lifting favored when it is large. Both methods of displacement can be considered using the approach outined here. However, lifting dominates compression of the overburden when the ratio of total length to depth is greater than 3 (Pollard and Johnson 1973). Approximately 80% of the fractures described by Murdoch and Slack (2002) had maximum lengths that were three or more times greater than their depth (Murdoch and Slack 2002, Fig. 4).

The fractures described by Murdoch and Slack (2002) appear to have dilated primarily by lifting their overburden, particularly relatively late in their growth. This assumption is made with full cognizance that the early history of growth, when the fractures are short relative to their depth, may be poorly represented by the analysis.

Mechanical Idealization

The analysis will assume that the ground over the fracture deforms as a thin, circular, elastic plate. A similar analogy was used by Pollard and Johnson (1973) and by Dyskin et al. (1999) to analyze shallow fractures. The use of the thin-plate analogy tacitly ignores changes in displacement with depth; that is, the aperture of the fracture is assumed to be equal to the vertical displacement of the ground surface. Sampling and excavation studies suggest that the thickness of material injected into a hydraulic fracture is proportional to the uplift of the ground surface over the fracture, and that the edge of the uplifted ground roughly overlies the edge of the fracture at depth (Murdoch and Slack 2002; Figs. 5 and 7). Moreover, the volume with which the ground has been displaced is roughly the same as the injected volume (Murdoch and Slack 2002, Fig. 12). As a result of these observations, the assumption that the ground over shallow hydraulic fractures flexed like a thin plate appears justified.

The analysis will determine the injection pressure, aperture, and length of the hydraulic fracture as functions of time. This will be done by using the thin-plate analogy to determine expressions for the aperture and the volume of a pressurized, static fracture. Linear elastic fracture mechanics will be used to derive an expression for the stress intensity factor, which will provide as a criterion that must be met to maintain propagation. The three equations for aperture, volume, and stress intensity will be solved simultaneously to determine the injection pressure, aperture, and length of the fracture. The volume of the fracture changes with time, and the analysis will be made transient by balancing the volume of the fracture (and associated leakage) with the volume

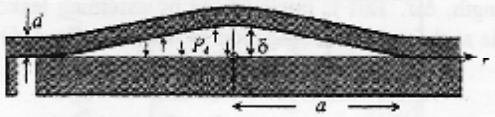

Fig. 2. Section view of the loading and terms used in the analysis. Radial symmetry is assumed.

of injected fluid. Methods for including the effects of leakoff and viscous dissipation within the fracture will also be presented; however, it will be shown that the effects of leakoff are negligible for the range of field conditions and treatment designs that are used as examples.

Analysis

The ground over a shallow hydraulic fracture is represented as a flay-lying, thin elastic plate of thickness d, modulus E, and Poisson's ratio ν. The plate is loaded by a uniform net pressure, or driving pressure P_d=(fluid pressure−overburden pressure) over a circular area of radius a (Fig. 2). The plate is assumed to be clamped at its outer edge, which means that both the displacement and the slope of the plate are zero at $r=a$ (Fig. 2).

The vertical displacement of the overburden δ, which is assumed to be equal to the fracture aperture, is given by Love (1927)

$$\delta(r)=\delta_0[1-(r/a)^2]^2 \tag{1}$$

where the displacement at the origin is

$$\delta_0=\frac{3P_d a^4}{16d^3E'} \tag{2}$$

Plane strain is assumed, and $E'=E/(1-\nu^2)$. Downward displacement of the lower fracture wall will be ignored (Perkins and Kern 1961).

The mode I stress intensity at the leading edge of a circular fracture in plane strain is (Williams 1984)

$$K_I^2=\frac{E'P_d}{2a}\int_0^a r[dc/da]dr \tag{3}$$

where the compliance c for the configuration in Fig. 2 is

$$c=\frac{3}{16d^3E'}a^4[1-(r/a)^2]^2 \tag{4}$$

It follows that the mode I stress intensity factor for this loading is

$$K_I=P_d a^2\left[\frac{3}{32d^3}\right]^{1/2} \tag{5}$$

The fracture is assumed to propagate under equilibrium conditions, which implies that the mode I stress intensity equals a critical value, K_{IC}, the fracture toughness, during propagation. Murdoch (1993a,b,c) showed that this approach is a viable method of predicting the behavior of hydraulic fractures created in silty clay during laboratory experiments, and Harison et al. (1994) concluded that fracture toughness of cohesive soil can be used to predict tensile fracturing in laboratory samples.

The use of K_{IC} as a propagation criterion overlooks the contribution of a mode II stress intensity, K_{II}, during propagation. Pollard and Holzhausen (1979) and Dyskin et al. (1999) showed that K_{II} will increase as two-dimensional rectangular fractures become closer to a free surface. Indeed, the increase in mode II stress intensity is one process that has been inferred to cause upward growth of shallow hydraulic fractures (Murdoch 1995). An expression for the mode II stress intensity of a shallow, *circular* fracture is, to my knowledge, unavailable. Dyskin et al. (1999, Table 1) show that for a long rectangular fracture K_{II} increases with a^2, just as K_I does. Assuming that a similar relation occurs for a circular fracture, then it appears that ignoring mode II may affect the magnitude of the stress intensity [by altering the constants in Eq. (5)] but it will not affect the form of the resulting analysis. The possibility that the fracture can curve upward, which is one consequence of K_{II}, has already been ignored so it seems reasonable to ignore the effect of K_{II} in the propagation criterion.

The analysis becomes a function of time by introducing a balance between the rate of injection and the volume of the fracture. This approach tacitly ignores dynamic effects during propagation, but propagation velocities that are a significant fraction of the speed of sound in the solid are required before dynamic effects are important. Nilson (1986) points out that viscous effects related to the injection of fluid during hydraulic fracturing will limit propagation rate so that dynamic effects are negligible. Assuming that an incompressible fluid is injected into the fracture at a constant rate Q, the time of injection is

$$t=(V_{leak}+V_{frx})/Q \tag{6}$$

where V_{leak}=volume that has leaked out through the walls of the fracture and V_{frx}=volume of the fracture itself.

It will be convenient to initially ignore volume losses due to leakoff and then include that process later. Integrating Eq. (1) gives the fracture volume

$$V_{frx}=\frac{\delta_0\pi a^2}{3} \tag{7}$$

Using Eqs. (2), (5), and (7) and solving for the driving pressure, radial length, and maximum aperture as functions of time gives

$$P_d=C_1 t^{-1/2} \tag{8a}$$

$$C_1=\frac{K_{IC}^{3/2}d^{3/4}}{Q^{1/2}E'^{1/2}}\left(\frac{32\pi}{6^{3/2}}\right)^{1/2}$$

$$a=C_2 t^{1/4} \tag{8b}$$

$$C_2=\frac{Q^{1/4}d^{3/8}E'^{1/4}}{K_{IC}^{1/4}}\left(\frac{24}{\pi^2}\right)^{1/8}$$

$$\delta_0=C_3 t^{1/2} \tag{8c}$$

$$C_3=\frac{K_{IC}^{1/2}Q^{1/2}}{d^{3/4}E'^{1/2}}\left(\frac{9}{2\pi 6^{1/2}}\right)^{1/2}$$

Viscous Losses in Fracture

Viscous dissipation will cause the pressure head to drop from the center to the outer edge of the fracture. This process can be included in a simplified manner (Perkins and Kern 1961) by assuming that at any given time the fracture is a disk-shaped slot of uniform aperture. The pressure of a Newtonian fluid flowing radially in the laminar regime is

$$p=p_i-\frac{6Q\mu}{\pi\delta^3}\ln\frac{r}{a_i} \tag{9}$$

where μ=slurry viscosity and p_i=pressure at the edge of the initial fracture, or starting slot, and a_i=radius of the slot. The

average pressure is obtained by integrating Eq. (9) over the area of the fracture and assuming that the radius of the fracture is much greater than the starting radius.

$$P_{ave}=p_i-\frac{3Q\mu}{\pi\delta_{ave}^3}[\ln(a/a_i)-1] \tag{10}$$

The average fracture aperture will be used in Eq. (10), so by integrating Eq. (1) over the fracture area we get

$$\delta_{ave}=\delta_0/3 \tag{11}$$

Friction losses in the pipe used for injection are ignored, so $p_i=p_{gs}+\gamma_{soil}d$, where p_{gs}=the pressure in the injection pipe at the ground surface. The driving pressure is defined as

$$P_d=P_{ave}-d\gamma_{soil} \tag{12}$$

Substituting into Eq. (10) and rearranging gives

$$p_{gs}=P_d+d(\gamma_{soil}-\gamma_{slurry})+\frac{81Q\mu}{\pi\delta_0^3}[\ln(a/a_i)-1] \tag{13}$$

Using Eq. (8) and neglecting leakoff gives the injection pressure as a function of time

$$p_{gs}=C_1t^{-1/2}+d(\gamma_{soil}-\gamma_{slurry})$$
$$-C_4C_3^{-3}t^{-3/2}\left[\frac{\ln(t)}{4}+\ln\left(\frac{C_2}{a_i}\right)-1\right] \tag{14}$$

where the effects of viscous losses are included in the last term, with

$$C_4=25.86Q\mu \tag{15}$$

Note that in the analysis presented above, the effects of viscous losses will change the pressure measured at the ground surface, but the quantities predicted in Eq. (8) will remain unchanged. This occurs because the mechanical analysis assumes the pressure in the fracture is uniform.

Leakoff

Leakage of injected fluid out through permeable fracture walls will result in a fracture that is shorter than it would be in an impermeable medium. This will increase the time required for a fracture to grow to a given length. Substituting Eqs. (7) and (2) into Eq. (6) gives the time to grow from a_1 to a as

$$t=\frac{V_{frx}+V_{leak}}{Q}=C_2a^4+\frac{8\pi C}{Q}\int_{a_1}^{a}r[t-\tau(r)]^{1/2}dr \tag{16a}$$

with

$$C_2=0.6413\frac{K_{IC}}{d^{3/2}E'Q} \tag{16b}$$

where $\tau(r)$=time when the leading edge of the fracture was at radius r and C=leakoff coefficient (Carter 1957). This equation is implicit in t and so it cannot be integrated directly. It is straightforward, however, to solve this equation iteratively. The procedure is to estimate an initial value for t and use it in Eq. (16) to calculate a revised value of t. The revised value is substituted back into Eq. (16), and this procedure is repeated until the relative error between successive estimates is less than a convergence criteria (0.001 was used in this work).

The growth of a fracture to length a was calculated by starting with an initial fracture of length a_1 and adding small increments of length, Δa. This is implemented by assuming leakoff is negligible at the start of propagation so that from Eq. (16)

$$t_2=C_2a_2^4 \tag{17}$$

is used for the first increment of growth to length $a_2=a_1+\Delta a$. The time required to grow by n increments to a_n is initially estimated by linear extrapolation using t_{n-1} and t_{n-2}. The initial estimate for t_n is used along with the calculations of a and t when the fracture length was shorter than a_n to integrate Eq. (16). The trapezoid method was used for the integration. This procedure gives the fracture length as a function of time. Driving pressure as a function of time is then obtained explicitly by rearranging Eq. (5), and the aperture follows from Eq. (2). Injection pressure is calculated using Eq. (13).

Application

The analysis will be calibrated by deriving appropriate values of C, E', and K_{IC} from field data. The calibrated model will be tested by comparing observed injection pressures and uplift or apertures values to transient predictions. The model will be further tested by using average values of E' and K_{IC} determined for a particular site to predict the maximum uplift and lengths of 16 fractures, and comparing those predictions to measurements made in the field.

Calibration

Calibration of the model requires estimating C, E', and K_{IC} for site conditions. It is possible to estimate these parameters from laboratory data. However, only a few measurements of K_{IC} of soil have been described (Murdoch 1993a,b,c; Harison et al. 1994), and a standard lab technique for making these measurements is unavailable.

An alternative is to estimate the parameters from tests of hydraulic fracturing in the field. Leakoff coefficients were estimated at several sites underlain by silty clay till by analyzing the record of injection pressure using methods similar to those described by Nolte (1989). Those estimates suggest that C is roughly 0.003 cm min$^{-1/2}$ when crosslinked guar gum is injected into silty clay glacial drift ($K\approx10^{-6}$ cm/s). This value indicates that V_{leak} is less than a few percent of V_{frx}. It seems reasonable to ignore the effects of leakoff when creating fractures of the size described by Murdoch and Slack (2002) with guar gum gel in clay-rich formations. Leakoff will be assumed to be zero in the remaining applications, although it probably will be important in some applications, such as when creating hydraulic fractures in formations that are more permeable than silty clay.

Elastic modulus and K_{IC} can be estimated from measurements of maximum uplift and injection pressure as a function of time. This was done by selecting several representative values of injection pressure as a function of time. This simple filtering was necessary because it allowed anomalies caused by field operations that are unrelated to the processes included in the analysis (e.g., stopping and restarting the injection pump) to be omitted. A parameter estimation scheme was used to obtain K_{IC} and E' that minimize the residual error between observed pressure and uplift and values predicted using Eq. (8). The minimization scheme was implemented using the Solver routine in *EXCEL*.

The approach described above was used to estimate K_{IC} and E' at a site underlain by a firm to stiff, CH to CL (Terzaghi and Peck 1967) silty clay vertisol near Beaumont, Tex. Standard prop-

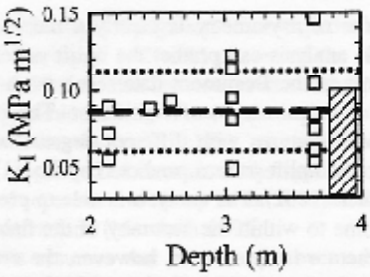

Fig. 3. Fracture toughness as a function of depth in Beaumont clay. Dashed line is the mean and dotted line is one standard deviation. The box on the right shows the range of toughness determined for a CL soil in the laboratory by Harison et al. (1994).

erties of this soil are described by Mahar and O'Neill (1983). The critical stress intensity, K_{IC}, appears to be independent of depth with an average of 0.071 MPa m$^{1/2}$, a standard deviation of 0.018 MPa m$^{1/2}$, and a coefficient of variation of 0.25 (Fig. 3).

Independent measurements of the fracture toughness of Beaumont clay were unavailable at the time of this writing, but there are two studies of generally similar materials that are noteworthy. Harison et al. (1994) measured the fracture toughness of a remolded CL soil in the laboratory and found that K_{IC} was 0.10 MPa m$^{1/2}$ at a water content of 10 wt % and decreased to 0.03 MPa m$^{1/2}$ at 20 wt % water. Their estimates show considerable variability, ranging over approximately 0.07 MPa m$^{1/2}$ for any particular water content. Murdoch (1993b) also found that K_{IC} of a CL silty clay decreased with water content, and his measurements were in the range of 0.01–0.05 MPa m$^{1/2}$ for volumetric water contents of 0.23–0.30. Contamination precluded making measurements of water content at the Beaumont site, but the hydraulic fractures were created within a meter of the water table (above and below), so the silty clay can be assumed to be saturated and the higher water contents given above would be appropriate for comparison.

It appears that the method described above for estimating fracture toughness from full-scale field data gives results that are similar to data obtained from laboratory tests on similar material (Fig. 3). It is possible that the field method may give slightly greater values of K_{IC} than the laboratory techniques do, although additional laboratory testing using soil from the field site would be required to evaluate this possibility.

Elastic modulus determined using the approach described above ranges from 2.5 to 17.6 MPa, and appears to be independent of depth (Fig. 4) for the depth range evaluated during the study. The average value is 9.7 MPa, standard deviation is 5.3 MPa, and the coefficient of variation is 0.55.

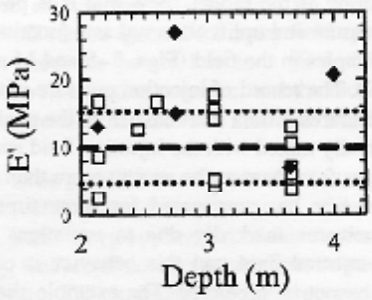

Fig. 4. Elastic modulus as a function of depth in Beaumont clay. Open squares are from this study (dashed line is the mean and dotted line is one standard deviation), filled diamonds are from Mahar and O'Neill (1983, Fig. 12).

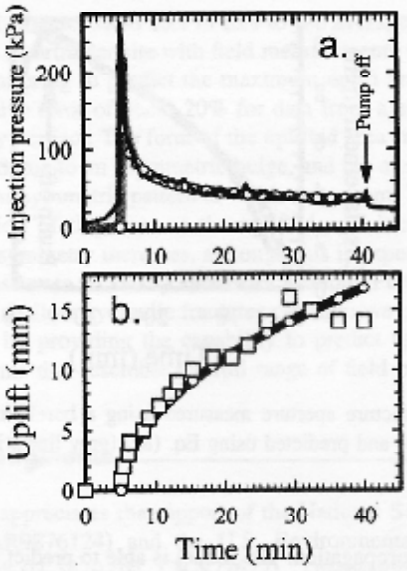

Fig. 5. (a) Injection pressure as a function of time from field observations (black line) and theoretical analysis (gray line with dots). (b) Uplift as a function of time from field observations (open symbols) and theoretical analysis. $K_{IC}=0.08$ Mpa m$^{1/2}$, $E'=45$ Mpa (gray line with dots).

Mahar and O'Neill (1983) determined the elastic modulus of Beaumont clay using several different field and laboratory methods. They found (Mahar and O'Neill 1983, Fig. 12) that estimates of elastic modulus ranged from approximately 7 to 27 MPa depending on the type of experimental method. Their data give a mean of 17.4 MPa, a standard deviation of 7.2 MPa, and a coefficient of variation of 0.41. The mean value obtained by Mahar and O'Neill is 1.8 times greater than the mean value obtained using hydraulic fracturing, however, there is considerable variation in both sets of measurements (Fig. 4).

Transient Data

The analysis presented above was used to predict aspects of the behavior of a fracture created at a depth of 1.83 m at a site underlain by a stiff to very stiff, CL (Terzaghi and Peck 1967) silty clay glacial drift (water content: 16%, void ratio: 0.5, wet unit weight: 21 kN/m^3, dry unit weight 17.9 kN/m^3) in Chicago, Ill. The fracture contained 0.74 m^3 of fracturing gel with an apparent viscosity of 180 cp and no sand. The injection rate was $Q=0.021$ m^3/min. The injection pressure was measured at the well head using a datalogger, and the displacement of the ground surface was measured at several locations using a leveling telescope.

Values of K_{IC} and E' were determined by minimizing the squared residual between pressure and uplift histories observed in the field and those predicted using Eqs. (8*a*), (13), (14), and (8*c*). This gives $K_{IC}=0.08$ MPa m$^{1/2}$ and $E'=45$ MPa.

The field data indicate that the injection pressure increases abruptly to 260 kPa when the pump is turned on at $t=5$ min [Fig. 5(a)], but then it decreases sharply and continues to decrease throughout the duration of injection. The model predicts the injection pressure to within approximately 10 kPa throughout the

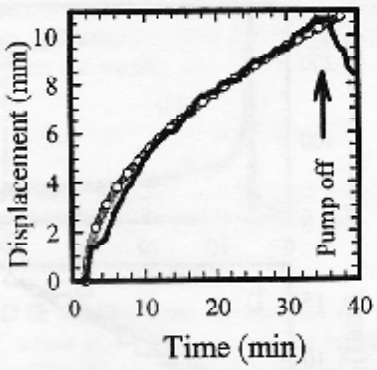

Fig. 6. Fracture aperture measured using a borehole extensometer (black line) and predicted using Eq. (8*c*) (gray line with dots).

period of propagation. The model is able to predict the maximum uplift within approximately 1.5 mm during most of the period of propagation [Fig. 5(b)]. Departures from the predicted values occur after 25 min, relatively late in the period of injection. This fracture was asymmetric with respect to the borehole, similar to Fig. 9(b) in Murdoch and Slack (2002), and the asymmetry probably contributed to departures from predicted values.

Fracture aperture has been measured directly in a few cases using a borehole extensometer, and the results of these measurements are remarkably similar to the form predicted by Eq. (8*c*). Observed apertures during the test described by Murdoch and Slack (2002) (their Fig. 7), for example, were used to estimate a value for C_2 using Eq. (8*c*). The analysis predicts (Fig. 6) the observed aperture to within 0.5 mm throughout growth of the fracture. It is noteworthy that this fracture was created with a piston pump, which produced a highly oscillatory pressure record that defied a meaningful interpretation using Eq. (8*a*). For this reason it was impossible to estimate K_{IC} and E for this example.

Fracture Form

An alternative method of testing the analysis is to compare the final forms of fractures observed in the field to those predicted by the analyses. This was done using the data from the Beaumont site, where average values of K_{IC} and E' (Figs. 3 and 4) were used with Eq. (8) to predict maximum uplifts and lengths of fractures. The relative errors [(predicted-observed)/observed] were calculated as a measure of how well the calibrated model could predict the uplift and length.

The results indicate that the mean relative error between the predicted and observed maximum uplift is −0.05, whereas the mean of the absolute value of the relative error is 0.19. The mean relative error between the predicted and observed length is 0.10, whereas the mean of the absolute value of this relative error is 0.30.

This suggests that, on average, the analysis underpredicted the uplift by about 5% and overpredicted the length by about 10% when average values of fracture toughness and modulus were used for the Beaumont data. However, the means of the absolute values of the relative errors are several times greater than the means of the relative errors themselves. This suggests that the error of any particular prediction was 20% for uplift and 30% for length, on average. The errors are both positive and negative, which is why the mean of the relative error is less than the mean of the absolute value of the error.

The degree of asymmetry is clearly a major factor affecting how well the analysis can predict the uplift pattern. Some of the greatest errors in the Beaumont data result from fractures where the degree of asymmetry was significant. The pattern of uplift observed over fractures with different degrees of symmetry are compared to the uplift pattern predicted by Eq. (1) given by Murdoch and Slack (2002). The analysis is able to predict the form of the uplift dome to within the accuracy of the field measurements when the fracture is symmetric, however, the error increases as the fracture becomes asymmetric (e.g., Murdoch and Slack 2002, Fig. 9).

Discussion

The analysis described here is able to predict essential details, such as the injection pressure, aperture, and length of hydraulic fractures from selected examples that are gently dipping and several times longer than their depth of initiation. This predictive capability offers insights into the creation of shallow hydraulic fractures, but it is important to keep in mind the limitations that have resulted from the assumptions required to formulate the analysis.

Hydraulic fractures were assumed to resemble a flat-lying circular disk and that only the radial length changes during growth, and this assumption limits the applicability to fractures that resemble this form. Hydraulic fractures that dip less than 20° and that have symmetries typical of those shown in Fig. 1(a) probably can be predicted with accuracies that are acceptable for field conditions. Most environmental implementations are best suited to hydraulic fractures that are gently dipping (Murdoch 1995; Murdoch et al. 1997), so the analysis is applicable to a useful form of fractures.

It appears that the analyses presented here can be used to estimate K_{IC} and E' by analyzing results of tests that stress relatively large regions (on the order of 10 m across) of material. Field methods for measuring K_{IC} in situ currently are unavailable, and field methods for estimating E' are limited to measurements made in borings that affect a relatively limited volume of material. As a result, it is difficult to validate the results of this application. It is possible that the technique described here for estimating E' by stressing a relatively large volume of soil may have applications for investigating possible changes in modulus with scale, or where other methods are unavailable or infeasible. It is important to point out, however, that the method described here for estimating K_{IC} and E' was developed to calibrate a model for predicting the growth of hydraulic fractures, and other uses for the analysis still need to be tested.

Applications of the model show that it is possible to predict injection pressure and uplift observed as a function of time during selected examples in the field (Figs. 3–5 and Murdoch and Slack 2002, Fig. 9). The record of injection pressure with time for some hydraulic fractures differs markedly from the analysis given here. Sand is typically mixed with the injection fluid and the proportion of sand ranges from zero at the start to more than 30% by volume after the fracture has propagated for some time. The injection pressure fluctuates markedly due to variations in rheology of sand-laden injected fluid and this behavior is omitted from the model and cannot be predicted. The example shown in Fig. 5(a) lacked sand in the injection fluid, so complications related to changing rheology were avoided.

During some field applications where sand is used in the injection fluid, the pressure decreases at a rate that is slower than predicted by the model, and in some cases, the pressure remains

nearly constant during propagation. One explanation of this behavior is that the liquid and solid phases of the slurry separate, with the liquid flowing into the narrow fracture tip and sand deposited slightly behind the tip. The increasing sand concentrations slightly behind the tip could inhibit propagation and result in behavior that resembled an increase in the apparent K_{IC} with time. The process of separation of slurry in the fracture tip is consistent with field observations (Murdoch 1995).

The analysis assumes that the material over a hydraulic fracture deflects like a thin plate, and this assumption will limit the applicability to fractures that are shallow relative to their diameter. It is possible to modify the analysis given here to consider deep, circular fractures where the displacements vary with depth by using analyses described by Sun (1969) and Dyskin et al. (1999). This would relax the restriction to shallow fractures, although it would still require the fracture to be shaped like a flat-lying circular disk.

The performance of geotechnical operations, such as permeability testing, grouting, or well drilling, can be hampered by hydraulic fractures that form unintentionally, and there is considerable interest in understanding how to predict fracturing during these operations. The analysis described here could be useful for making such predictions, but it would require some estimate of the size of the initial fracture intersected by the borehole. It is important to point out, however, that the purpose of this analysis was to predict aspects of hydraulic fractures that were created intentionally, and the effectiveness with which the analysis can predict the onset of fracturing is unclear.

Many of the limitations of this analysis result from the need to specify the geometry of the fracture in order to obtain a closed form expression; the analysis is unable to realistically predict the propagation path of a shallow hydraulic fracture. To lift these limitations will require a three-dimensional analysis where the hydraulic fracture can propagate out of its original plane and become asymmetric with respect to its parent borehole (Carter et al. 2000). Developing analyses with the ability to predict the growth of hydraulic fractures with realistic forms, which avoid the assumptions needed to simplify Figs. 1(a and b), is the challenge that should guide future efforts to understand the growth of shallow hydraulic fractures.

Conclusions

A theoretical analysis based on linear elastic fracture mechanics has been developed to predict the behavior of a shallow, flat-lying circular hydraulic fracture. The analysis assumes equilibrium propagation and accounts for fluid losses out through the wall of the fracture. Those losses are small when fractures of the size described here are created in silty clay, so it appears that the effects of leakoff can be ignored for many field applications. This simplification produces power functions [Eqs. (8)] that predict uplift (or aperture), injection pressure, and the radial length of the fracture as functions of time, elastic modulus, and fracture toughness.

It appears to be possible to estimate elastic modulus and fracture toughness of soil using measurements of injection pressure and uplift. A preliminary application of this method gives values of E' and K_{IC} that are similar to measurements made using independent methods. This suggests that the proposed model can be calibrated either with results from laboratory tests or with analysis of preliminary field data obtained during the creation of hydraulic fractures. Moreover, it may be possible to use the results of hydraulic fracturing tests to estimate properties of shallow formations.

The analysis presented here is able to use average values of E and K_{IC} for a particular site with field measurements made during routine monitoring to predict the maximum uplift and the radius with a relative error of about 20% for data from a site underlain by silty clay vertisol. The form of the uplifted area ranges from a symmetric dome to an asymmetric bulge, and the analysis is able to predict the symmetric pattern to within a few mm. The errors in the prediction of the form of the uplifted area increase as the degree of asymmetry increases, although this is expected because the model assumes an axially symmetric loading. Future efforts to understand shallow hydraulic fractures can improve on the results given here by providing the capability to predict the growth of fracture forms that resemble the full range of field observations.

Acknowledgments

The writer appreciates the support of the National Science Foundation (EAR9876124) and the U.S. Environmental Protection Agency (68-03-3379-08; CR-822677). Discussions with Bill Slack were invaluable throughout the preparation of this manuscript. The writer also appreciates the suggestions of Leonid Germanovich.

Notation

The following symbols are used in this paper:

a = radial length of fracture;
a_i = radius of initial fracture or starting slot;
C = leakoff coefficient;
c = compliance;
d = depth;
E = elastic modulus;
E' = $E/(1-\nu^2)$;
K_{IC} = critical mode I stress intensity;
K_I, K_{II} = mode I and II stress intensity;
P_d = driving pressure;
P_{gs} = injection pressure at the ground surface;
p = pressure in the fracture;
p_{ave} = average pressure in the fracture;
p_i = pressure at the leading edge of the starting slot;
Q = volumetric injection rate;
r = radial coordinate;
t = time;
V_{frx} = volume of fluid in the fracture;
V_{leak} = volume of fluid that has leaked out of fracture;
γ_{slurry} = unit weight of slurry injected into fracture;
γ_{soil} = unit weight of soil;
δ = uplift or aperture;
δ_{ave} = average aperture or uplift;
δ_0 = maximum uplift or aperture;
μ = dynamic viscosity; and
ν = Poisson's ratio.

References

Bjerrum, L., Nash, J. K. L., Kennard, R. M., and Gibson, R. E. (1972). "Hydraulic fracturing in field permeability testing." *Geotechnique*, 22, 319–332.

Caron, C. (1982). "The state of grouting in the 1980s." *Proc., Conf. on Grouting in Geotechnical Engineering*, W. H. Baker, ed., ASCE, New York, 346–358.

Carter, B. J., Desroches, J., Ingraffea, A. R., and Wawrzynek, P. A. (2000). "Simulating fully 3D hydraulic fracturing," *Modeling in geomechanics*, M. Zaman, J. R. Booker, and G. Gioda, eds., Wiley, New York.

Carter, R. D., Appendix to paper by Howard, C. C. and Fast, C. R. (1957). "Optimum fluid characteristics for fracture extension." *Drilling Prod. Prac.*, API, 267.

Chandler, S. C. (1997). "Lense grouting with fiber admixture to reinforce soil." *Grouting: Compaction, remediation and testing*, C. Vipulanandan, ed., ASCE, New York, 147–156.

Dyskin, A. V., Germanovich, L. N., and Ustinov, K. B. (1999). "Asymptotic analysis of crack interaction with free boundary." *Int. J. Solids Struct.*, 37(6), 857–886.

Gidley, J. L., Holditch, S. A., Nierode, D. E., and Veatch, R. W. (1989). *Recent advances in hydraulic fracturing*, Society Petroleum Engineers Monograph, 452.

Harison, J. A., Hardin, B. O., and Mahboub, K. (1994). "Fracture toughness of compacted cohesive soils using a ring test." *J. Geotech. Eng.*, 120(5), 872–891.

Love, A. E. H. (1927). *A treatise on the mathmatical theory of elasticity*, Dover, New York, 481.

Mahar, L. J., and O'Neill, M. W. (1983). "Geotechnical characterization of desiccated clay." *J. Geotech. Eng.*, 109(1), 56–71.

Morgenstern, N. R., and Vaughan, P. R. (1963). "Some observations on allowable grouting pressures." *Proc., Conf. Grouts and Drill. Muds*, Institute of Civil Engineering, London., 36–42.

Morris, P. H., Graham, J., and Williams, D. J. (1994). "Crack depths in drying clay using fracture mechanics." *Fracture mechanics applied to geotechnical engineering*, L. E. Vallejo and R. L. Liang, eds., ASCE, New York, 40–53.

Murdoch, L. C. (1988). "Innovative delivery and recovery using hydraulic fracturing." *Proc., 14th Annual USEPA Research Symposium*, 615.

Murdoch, L. C. (1989). "A field test of hydraulically fracturing glacial till." *Proc., 15th Annual USEPA Research Symposium*, Cincinnati.

Murdoch, L. C. (1991). "The hydraulic fracturing of soil." PhD dissertation, Univ. of Cincinnati.

Murdoch, L. C. (1993a). "Hydraulic fracturing of soil during laboratory experiments: methods and observations." *Geotechnique*, 43(2), 255–265.

Murdoch, L. C. (1993b). "Hydraulic fracturing of soil during laboratory experiments: propagation." *Geotechnique*, 43(2), 265–276.

Murdoch, L. C. (1993c). "Hydraulic fracturing of soil during laboratory experiments: theoretical analysis." *Geotechnique*, 43(2), 277–287.

Murdoch, L. C. (1995). "Forms of hydraulic fractures created during a field test in fine-grained glacial drift." *Q. J. Eng. Geol.*, 28, 23–35.

Murdoch, L. C. (2000). "Remediation of organic chemicals in the vadose zone." *Vadose Zone, Science and Technology Solutions*, B. B. Looney and R. W. Falta, eds., Battelle, 949–1237.

Murdoch, L. C., and Slack, W. W. (2002). "Forms of hydraulic fractures in shallow fine-grained formations." *J. Geotech. Geoenviron. Eng.*, 128(6), 479–487.

Murdoch, L. C., Slack, W., Siegrist, R., Vesper, S., and Meiggs, T. (1997). "Advanced hydraulic fracturing methods to create in situ reactive barriers." *Proc., Int. Containment Technology Conf. and Exhibition*, St. Petersburg, FL, sponsored by DOE and USEPA.

Murdoch, L. C., Wilson, D., Savage, K., Slack, W., and Uber, J. (1995). *Alternative methods for fluid delivery and recovery*, USEPA/625/R-94/003.

Nilson, R. H. (1986). "An integral method for predicting hydraulic fracture propagation driven by gases or liquids." *Int. J. Numer. Methods Geomech.*, 10, 191–211.

Nolte, K. G. (1989). "Fracturing-pressure analysis." *Recent advances in hydraulic fracturing*, J. L. Gidley, ed., *Soc. Petrol. Eng. Monograph*, 12, 297–316.

Perkins, T. K., and Kern, L. R. (1961). "Widths of hydraulic fractures." *J. Pet. Technol.*, 937–949.

Pollard, D. D. (1973). "Derivation and evaluation of a mechanical model for sheet intrusions." *Tectonophysics*, 19, 233–269.

Pollard, D. D. (1978). "Forms of hydraulic fractures as deduced from field studies of sheet intrusions." *United States Symposium of Rock Mechanics*, Y. S. Kim, ed., Univ. of Nevada, Reno, Nev., 1–9.

Pollard, D. D., and Holzhausen, G. (1979). "On the mechanical interaction between a fluid-filled fracture and the earth's surface." *Tectonophysics*, 53, 27-57.

Pollard, D. D., and Johnson, A. M. (1973). "Mechanics of growth of some laccolithic intrusions in the Henry Mountains, Utah, II." *Tectonophysics*, 18, 311–354.

Sun, R. J. (1969). "Theoretical size of hydraulically induced fractures and corresponding surface uplift in an idealized medium." *J. Geophys. Res.*, 74, 5995–6011.

Terzaghi, K., and Peck, R. B. (1967). *Soil mechanics in engineering practice*, Wiley, New York, 729

Vallejo, L. E., and Liang, R. L., eds. (1994). *Fracture mechanics applied to geotechnical engineering*, ASCE, New York.

Veatch, R. W. (1983a). "Overview of current hydraulic fracturing design and treatment technology—Part 1." *J. Pet. Technol.*, 677–687.

Veatch, R. W. (1983b). "Overview of current hydraulic fracturing design and treatment technology—Part 2." *J. Pet. Technol.*, 853–863.

Williams, J. G. (1984). *Fracture mechanics of polymers*, Wiley, New York, 302.

Wong, H. Y., and Farmer, I. W. (1973). "Hydrofracture mechanisms in rock during pressure grouting." *Rock Mech.*, 5, 21–41.